Sciencexpress Report

# The Dark Side of the Rings of Uranus

Imke de Pater,[1]* H. B. Hammel,[2] Mark R. Showalter,[3] Marcos A. van Dam[4]

[1]Astronomy Department, 601 Campbell Hall, University of California, Berkeley, CA 94720, USA. [2]Space Science Institute, 4750 Walnut Street, Suite 205, Boulder, CO 80301, USA. [3]SETI Institute, 515 North Whisman Road, Mountain View, CA 94043, USA. [4]W. M. Keck Observatory, 65-1120 Mamalahoa Highway, Kamuela, HI 96743, USA.

*To whom correspondence should be addressed. E-mail: imke@astron.berkeley.edu

**The rings of Uranus are oriented edge-on to Earth in 2007 for the first time since their 1977 discovery. This provides a rare opportunity to observe their dark (unlit) side, where dense rings darken to near invisibility, but faint rings become much brighter. We present a ground-based infrared image of the unlit side of the rings that shows that the system has changed dramatically since previous views. A broad cloud of faint material permeates the system, but is not correlated with the well-known narrow rings or with the embedded dust belts imaged by Voyager. Although some differences can be explained by the unusual viewing angle, we conclude that the dust distribution within the system has changed significantly since the 1986 Voyager spacecraft encounter and occurs on much larger scales than has been seen in other planetary systems.**

A planet's axial tilt causes an Earth-bound observer to see varying views as the planet travels around the Sun. Uranus has a tilt of 98°, so it presents extreme changes in viewing geometry during its 84-year orbit. The Voyager 2 encounter with Uranus in 1986 occurred near that planet's southern summer solstice—with its south pole pointed almost directly toward the Sun—so the rings were face-on and fully illuminated as Voyager approached (*1*). Twice during a Uranian year, the rings appear edge-on for a brief period, referred to as a ring plane crossing (RPX). We are currently in the midst of the first RPX since the rings were discovered in 1977 (Fig. 1) (*2*).

The RPX offers a rare opportunity to study features not usually observable, as exemplified by Saturn's RPX in 1995 (*3*–*5*). In particular, observations of the "dark" or unlit side of the rings—when the Sun and the Earth are on opposite sides of the ring plane—provide the chance to characterize faint, optically thin regions. As the rings' opening angle *B* decreases, optically thin rings brighten as 1/sin(*B*), while optically thick rings fade due to mutual shadowing and obscuration of particles.

On UT 28 May 2007, we obtained an infrared image of the dark side of the ring system with the 10-m W. M. Keck II telescope. We used the near-infrared camera NIRC2, coupled to the adaptive optics (AO) system. Thirty 1-min images were combined. The pixel size was ~ 146 km (0.01″), yielding an effective resolution of 660 km. Absolute photometry was bootstrapped from Uranus itself, using data obtained in July 2004 (*8*, *9*). Methane and hydrogen gas absorb sunlight in K' band (2.2 μm), so Uranus is relatively dark, allowing ring material to be traced very close to the planet (Fig. 2). We did not detect the recently discovered outer ring system (*6*, *7*) due to the relatively short exposure time.

The rings show significant changes from the lit side (Fig. 3). The ε ring's pericenter was oriented near the northern tip or "ansa" in all three epochs. The ε ring is narrowest at pericenter, so its smaller area results in a brightness minimum. This allows easier characterization of the (much fainter) inner rings. Because the ε ring's southern tip was ~ 2.5 times brighter in 2004, and 4 times brighter in 2006 (*8*), we focus our discussion here on the northern tip of the rings.

The radial extent of the rings appears much smaller in 2007. The ε ring, the dominant feature in observations prior to 2006 (*6*, *7*, *9*–*13*), is completely absent. This ring had begun to fade in 2006 (Fig. 3). In May 2007, the brightest part of the ring system is a feature referred to as the ζ ring (*14*). It has remained ambiguous whether this feature is related to the faint band of dust, R/1986 U 2, which was seen in a single Voyager image. The ring system is also exceptionally bright near ring η, which was already the brightest region on the northern ansa in 2006 (Fig. 3).

Radial scans through the images (Fig. 3) show that the ε ring has been fading rapidly year by year (Fig. 4A). The ζ ring, on the other hand, increased in brightness by ~ 2.5 between 2004 and 2006, as is expected for an optically thin ring. Overall, most rings interior to ε brightened between 2004 and 2006, though only by a factor ~ 1.5 at most (*8*). Our 2007 profile differs markedly. On the unlit side of the optically thick main rings (4, 5, 6, α, β, η, γ, δ, ε), the only detectable light is that which either gets transmitted through from the lit side or is reflected from the ring's edge. Thus, these rings essentially disappear, and the reflectivity will be dominated by light scattered through optically thin regions of the system.

A detailed comparison of the profiles (Fig. 4A), however, is complicated by the fact that the 2007 profile is edge-on, so all the rings are superposed atop each other. To extract the radial distribution from these scans, we have applied an "onion-peel" deconvolution to the 15-pixel-wide scans (Fig. 2, red profiles). This technique has been successfully applied to a variety of rings in the past (*5*, *15*, *16*). Starting from the outer edge, the intensity of the outermost zone is determined and subtracted from the entire scan, after which the intensity of the next zone inward is determined, and so on.

The deconvolved profile from 2007 (Fig. 4B) is compared to the 2004 data and a much finer-resolution profile obtained by Voyager (*8*). This backscattered geometry emphasizes the larger (> cm) bodies within the system. We describe lighting geometry by the phase angle ϕ, the Sun-target-observer angle, which is near zero for all Earth-based observations. The profile from 2004 is a close match to the Voyager data, except for its coarser resolution. The 2007 profile, however, looks very different. The brightest feature is now ring η, followed closely by the broad, inner ring ζ.

Our new observations probe optically thin sheets of material. Elsewhere in the Solar System, optically thin rings are almost always dominated by micron-sized dust, so we may be seeing faint dust clouds surrounding the main rings of Uranus. Dust can be distinguished from larger bodies because it is strongly forward-scattering. When Voyager passed Uranus and looked back toward the Sun (high ϕ), extensive lanes of dust were seen throughout the system (Fig. 4C). One other image taken near Voyager's RPX detected a faint, interior ring R/1986 U 2.

The Voyager profiles (Fig. 4, B and C) look very different from ours, but a few features clearly correspond to known rings. Stellar occultations have revealed that two uranian rings have broad, optically thin components (*17*): ring η has a 55-km outward extension and the δ has a 12-km inward extension. The η ring's extension provides a natural explanation for its rapid growth in brightness as *B* decreases. Furthermore, Fig. 4C shows a subtle inflection closely aligned with ring δ, suggesting that its optically thin companion is glowing brighter at small *B*. Ring λ illustrates how a dusty ring should appear in our data (Fig. 4C). It is visible, but at a level ~ 150 times fainter than in the high-phase Voyager image. Such a ratio is compatible with the typical light-scattering properties of micron-sized dust. A broad feature at 43,000 km could also be related to dust seen by Voyager, but this feature remains somewhat ambiguous in our data because it was only detected on the south ansa (Fig. 2).

Many of the other ring components are difficult to reconcile with known rings. If such features are long-term members of the system, then they somehow escaped detection. Consider the region near 45,000 km, which is nearly devoid of dust according to Voyager, but is ~ half as bright as the η ring in our profile. One can devise an optically thin, backscattering population that fits the data, but extensive imaging by Voyager revealed no such population.

Even stranger is the ζ ring, which shifted radially from the Voyager epoch to the present. Because of the different phase angles, one cannot make any conclusive inferences about the particle sizes. Nevertheless, we require a broad, backscattering population centered at 40,000 km and an overlapping, slightly less backscattering population shifted inward by several thousand km. Such an explanation seems rather ad hoc, and it is difficult to understand how particles of slightly different sizes and scattering properties could become spatially segregated.

A simpler alternative is that the faint material we see is indeed dust, but that its radial distribution has changed since 1986, in fact much more dramatically than was suggested a year ago (*9*). One usually assumes that ring systems are static, but we now have several counterexamples. At Saturn, the D ring has changed substantially from the Voyager epoch (1980–1981) to the present (*18*) and the F ring also shows numerous changes (*19*). At Neptune, the pattern of dusty arcs in the Adams ring is very different now compared to Voyager's first images in 1989 (*20*, *21*). We conclude that changes in dusty rings over ~ 20-year time scales are common. The changes seen in Uranus's ring system, however, are much larger in scale than anything seen previously.

Changes over year-to-decade time scales are dynamically plausible because the dust populations we see represent extremely tiny amounts of material, and the orbits of small dust grains evolve rapidly in response to non-gravitational forces (e.g., Poynting-Robertson and plasma drag, Lorentz forces) (*22*). The rings were once expected to represent a steady state between dust creation and removal processes. However, we now realize that these states are far from steady, and may be dominated by infrequent events, such as large impacts, that inject highly visible quantities of dust, as has been discussed for Saturn's A ring (*23*).

**References and Notes**


1. B. A. Smith *et al.*, *Science* **233**, 43 (1986).
2. J. L. Elliot, E. W. Dunham, D. J. Mink, *Nature* **267**, 328 (1977).
3. P. D. Nicholson *et al.*, *Science* **272**, 453 (1996).
4. G. Verbanac, I. de Pater, M. Showalter, J. J. Lissauer, *Icarus* **174**, 241 (2005).
5. I. de Pater, S. Martin, M. R. Showalter, *Icarus* **172**, 446 (2004).
6. M. R. Showalter, J. J. Lissauer, *Science* **311**, 973 (2006).

7. I. de Pater, H. B. Hammel, S. G. Gibbard, M. R. Showalter, *Science* **312**, 92 (2006).
8. Materials and methods are available as supporting material on *Science* Online.
9. I. de Pater, S. G. Gibbard, H. B. Hammel, *Icarus* **180**, 186 (2006).
10. S. G. Gibbard, I. de Pater, H. B. Hammel, *Icarus* **174**, 253 (2005).
11. I. de Pater *et al.*, *Icarus* **160**, 359 (2002).
12. K. Matthews, G. Neugebauer, P. D. Nicholson, *Icarus* **52**, 126 (1982).
13. E. Karkoschka, *Icarus* **151**, 51 (2001).
14. The IAU definition of the ζ ring identifies the ring with R/1986 U 2, but uses the location and extent of the ζ ring as determined in (*9*); see http://planetarynames.wr.usgs.gov/append8.html
15. M. R. Showalter, J. A. Burns, J. N. Cuzzi, *Icarus* **69**, 458 (1987).
16. I. de Pater *et al.*, *Icarus* **138**, 214 (1999).
17. R. G. French, P. D. Nicholson, C. C. Porco, E. A. Marouf, in *Uranus*, Eds. J. T. Bergstrahl, E. D. Miner, and M. S. Matthews, pp. 327 (1991).
18. M. M. Hedman *et al.*, *Icarus* **188** (2007).
19. M. R. Showalter, *Icarus* **171**, 356 (2004).
20. C. Dumas, R. J. Terrile, B. A. Smith, G. Schneider, E. E. Becklin, *Nature* **400**, 733 (1999).
21. I. de Pater *et al.*, *Icarus* **174**, 263 (2005).
22. J. A. Burns *et al.*, in *Jupiter: The Planet, Satellites and Magnetosphere*, F. Bagenal, Ed. Cambridge University Press, pp. 241 (2004).
23. L. W. Esposito *et al.*, *Science* **307**, 1251 (2005).


24. We thank E. M. Johansson, P. J. Stomski Jr., R. J. Sumner, J. C. Y. Chin, P. L. Wizinowich at the W. M. Keck Observatory for upgrading the adaptive optics system. This work was funded by the National Science Foundation and Technology Center for Adaptive Optics, managed by the University of California at Santa Cruz under cooperative agreement No. AST-9876783. The W. M. Keck Observatory is operated as a scientific partnership among the California Institute of Technology, the University of California and the National Aeronautics and Space Administration, and was built with financial support of the W. M. Keck Foundation. Further support was provided by NASA grants NNX07AK70G (IdP), NNX06AD12G and NNG06GI25G (HBH), and NNX06AB98G (MRS).


**Supporting Online Material**

www.sciencemag.org/cgi/content/full/1148103/DC1

Materials and Methods

Fig. S1

References


20 July 2007; accepted 16 August 2007

Published online 23 August 2007; 10.1126/science.1148103

Include this information when citing this paper.


**Fig. 1.** Uranus-centered latitude of Earth and Sun during 2007 and early 2008. Earth crosses the ring plane three times: 3 May 2007, 16 August 2007, and 20 February 2008. The Sun crosses the ring plane on 7 December 2007 (equinox). Shaded regions indicate the times when the Earth and Sun are on opposite sides of the ring plane (i.e., on opposite sides of 0° latitude), providing a rare Earth-based look at the unlit side of the rings. The date of our image is indicated.

**Fig. 2.** The dark side of the rings of Uranus, as imaged by Keck adaptive optics. The ring plane is oriented horizontally, so celestial north points toward the right as indicated by the compass rose. Below the figure are profiles of ring intensity vs. projected radial distance. Horizontal white bars indicate the approximate radial extent of these profiles. Two versions of each profile are shown, one integrated over three rows of pixels (black) and the other over 15 rows (red). The broader integral captures more of the rings' light but shows somewhat less detail. The y-axis is "VIF" or vertically-integrated *I/F*. Here *I/F* is a dimensionless quantity, where *I* is intensity and $\pi F$ is the solar flux density. Note that the scales for VIF differ for the two integrals, with the black profile's scale shown at left and the red profile's scale shown at right.

**Fig. 3.** Comparison of the lit and unlit sides of the rings of Uranus. (**A**) The lit side in early July 2004, when the ring opening angle to Earth $B = 11^{\circ}$, and the angle $B_o$ to the Sun = $13.2^{\circ}$ (*5*). (**B**) The lit side on 1 August 2006 when $B = 3.6^{\circ}$ and $B_o = 5.2^{\circ}$. (**C**) The unlit side on 28 May 2007 when $B = 0.7^{\circ}$ and $B_o = 2.0^{\circ}$. The dotted lines show the position of rings ε (upper line) and ζ (lower line). The pericenter of ε was near the tip of the ring in 2006, at ~11 o'clock in 2004, and at ~2 o'clock position in 2007.

**Fig. 4.** (**A**) Radial profiles through the northern ansa of the main ring system (from Fig. 3). (**B**) Comparison of the deconvolved (i.e., onion-peeled) radial profile of 2007, averaged over both north and south sides (red; smoothed radially over ~ 650 km), with the northern profile from 2004 (cyan), and the Voyager profile in backscattered light (black). We shifted the Voyager ε ring to match the Keck profile, compensating for its large eccentricity. The left axis shows the *I/F* normal to the ring plane of the 2007 profile. The axis on the right side shows the measured *I/F* for the 2004 data. The scale for the Voyager data is arbitrary (and off-scale for ε). (**C**) Comparison of the deconvolved radial profile of 2007 (red; scale on left axis) with the Voyager profile in forward-scattered light from image 26852.19 (black; scale on right axis) and the Voyager profile of the R/1986 U 2 from image

26846.50 (blue, scale on left axis). The Voyager data were smoothed to match the Keck pixel size.

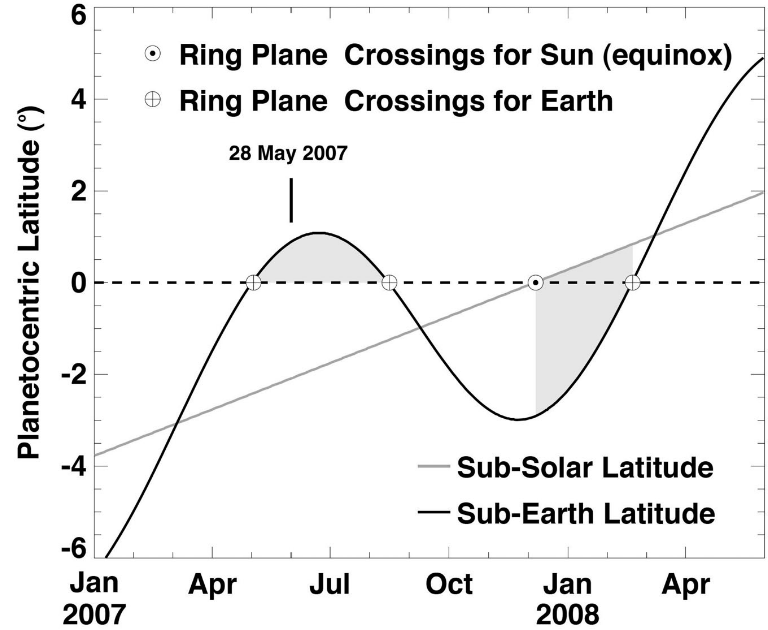

Ring Plane Crossings for Sun (equinox)
Ring Plane Crossings for Earth
28 May 2007
Planetocentric Latitude (°)
6
4
2
0
-2
-4
-6
Sub-Solar Latitude
Sub-Earth Latitude
Jan 2007
Apr
Jul
Oct
Jan 2008
Apr

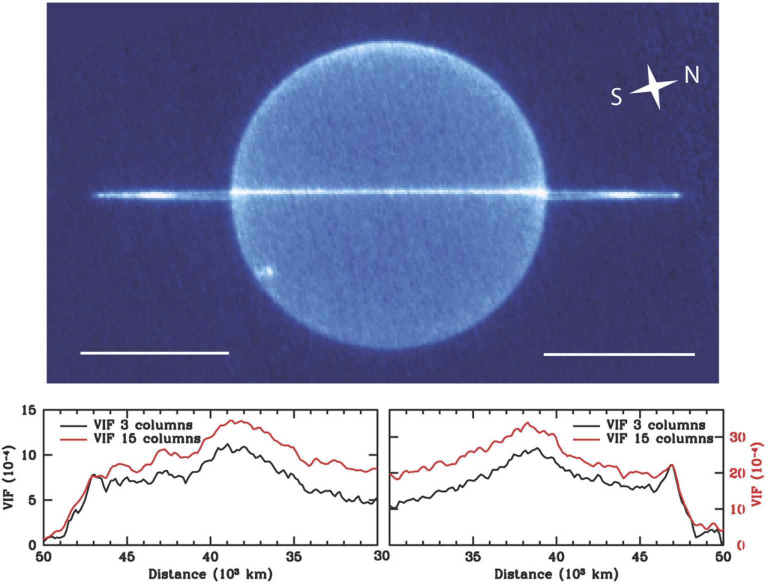
S
N
VIF 3 columns
VIF 15 columns
VIF (10⁻⁴)
15
10
5
0
50
45
40
35
30
Distance (10³ km)
VIF 3 columns
VIF 15 columns
30
20
10
0
VIF (10⁻⁴)
30
35
40
45
50
Distance (10³ km)

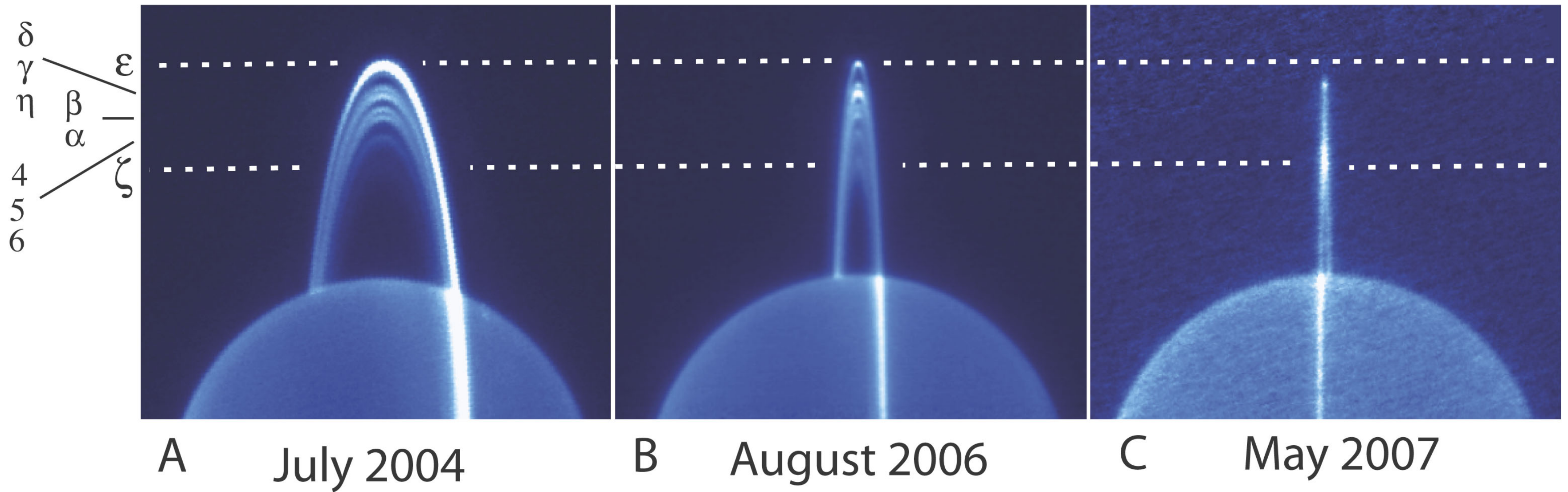
δ
γ
η
β
α
4
5
6
ε
ζ
A
July 2004
B
August 2006
C
May 2007

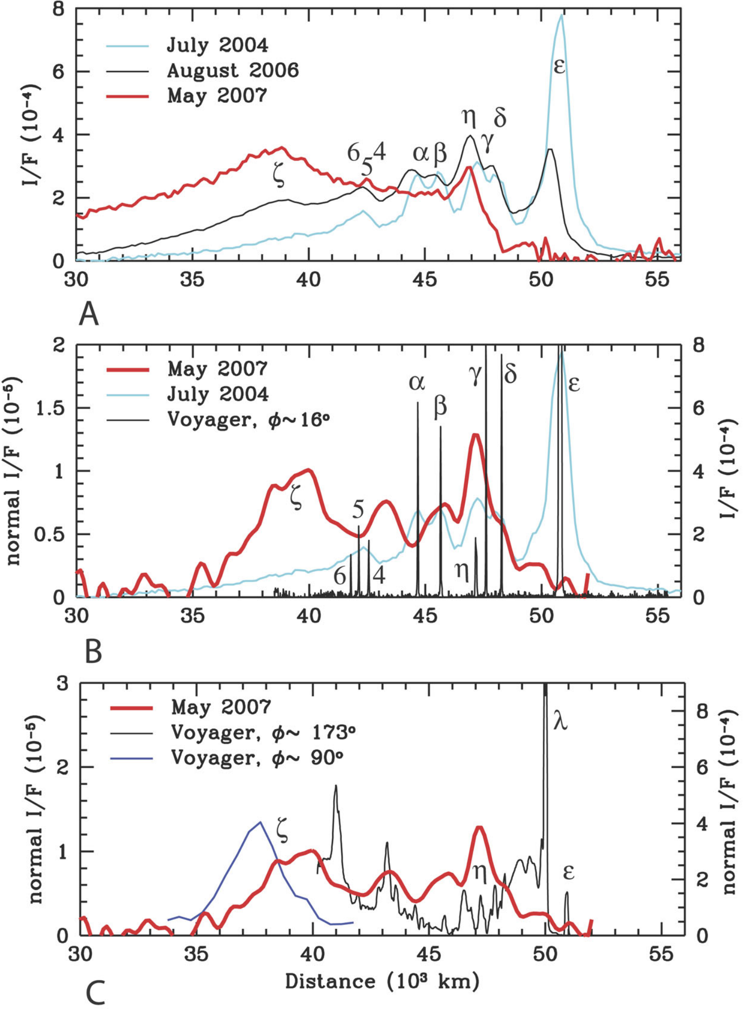

July 2004
August 2006
May 2007
I/F (10⁻⁴)
ζ
6 5 4
α β
η γ δ
ε
A
May 2007
July 2004
Voyager, φ~16°
normal I/F (10⁻⁵)
I/F (10⁻⁴)
B
May 2007
Voyager, φ~ 173°
Voyager, φ~ 90°
λ
normal I/F (10⁻⁵)
normal I/F (10⁻⁴)
Distance (10³ km)
C